EUROPEAN ORGANISATION FOR PARTICLE PHYSICS

CERN-PPE/93-155
August 23, 1993

Measurement of $\Gamma(Z^0 \to b\bar{b})/\Gamma(Z^0 \to \text{hadrons})$ using impact parameters and leptons

The OPAL Collaboration

Abstract

A measurement of $\Gamma_{b\bar{b}}/\Gamma_{had} \equiv \Gamma(Z^0 \to b\bar{b})/\Gamma(Z^0 \to \text{hadrons})$ is presented using a "mixed tag" method involving the identification of $Z^0 \to b\bar{b}$ events by two different techniques. The first uses the large impact parameter of tracks emerging from the decay of b-flavoured hadrons and the second their semi-leptonic decay. The identification efficiencies are measured from the data using all possible combinations of the two tags in opposite hemispheres. The method is therefore insensitive to Monte Carlo modelling of bottom quark production and of b-flavoured hadron production and decay properties, and depends only weakly on the simulation of the detector. The data sample collected by OPAL at LEP in 1990 and 1991 is considered. The result is:

$$\frac{\Gamma_{b\bar{b}}}{\Gamma_{had}} = 0.218 \pm 0.006\ (\text{stat}) \pm 0.007\ (\text{syst}) \pm 0.007\ (\Gamma_{c\bar{c}}/\Gamma_{had})\ ,$$

where the systematic uncertainty due to the charm quark partial width has been separated from the other systematic uncertainties. Combination with previous OPAL measurements gives:

$$\frac{\Gamma_{b\bar{b}}}{\Gamma_{had}} = 0.220 \pm 0.004\ (\text{stat}) \pm 0.006\ (\text{syst}) \pm 0.006\ (\Gamma_{c\bar{c}}/\Gamma_{had})\ .$$

(Submitted to Zeitschrift für Physik C)

The OPAL Collaboration

R. Akers[16], G. Alexander[23], J. Allison[16], K.J. Anderson[9], S. Arcelli[2], A. Astbury[28], D. Axen[29], G. Azuelos[18,a], J.T.M. Baines[16], A.H. Ball[17], J. Banks[16], R.J. Barlow[16], S. Barnett[16], R. Bartoldus[3], J.R. Batley[5], G. Beaudoin[18], A. Beck[23], G.A. Beck[13], J. Becker[10], C. Beeston[16], T. Behnke[27], K.W. Bell[20], G. Bella[23], P. Bentkowski[18], P. Berlich[10], S. Bethke[11], O. Biebel[3], I.J. Bloodworth[1], P. Bock[11], B. Boden[3], H.M. Bosch[11], M. Boutemeur[18], H. Breuker[8,b], P. Bright-Thomas[25], R.M. Brown[20], A. Buijs[8], H.J. Burckhart[8], C. Burgard[27], P. Capiluppi[2], R.K. Carnegie[6], A.A. Carter[13], J.R. Carter[5], C.Y. Chang[17], D.G. Charlton[8], S.L. Chu[4], P.E.L. Clarke[15], J.C. Clayton[1], I. Cohen[23], J.E. Conboy[15], M. Cooper[22], M. Coupland[14], M. Cuffiani[2], S. Dado[22], G.M. Dallavalle[2], S.J. De Jong[13], L.A. del Pozo[5], H. Deng[17], A. Dieckmann[11], M. Dittmar[4], M.S. Dixit[7], E. do Couto e Silva[12], J.E. Duboscq[8], E. Duchovni[26], G. Duckeck[11], I.P. Duerdoth[16], D.J.P. Dumas[6], P.A. Elcombe[5], P.G. Estabrooks[6], E. Etzion[23], H.G. Evans[9], F. Fabbri[2], B. Fabbro[21], M. Fierro[2], M. Fincke-Keeler[28], H.M. Fischer[3], D.G. Fong[17], M. Foucher[17], A. Gaidot[21], J.W. Gary[4], J. Gascon[18], N.I. Geddes[20], C. Geich-Gimbel[3], S.W. Gensler[9], F.X. Gentit[21], G. Giacomelli[2], R. Giacomelli[2], V. Gibson[5], W.R. Gibson[13], J.D. Gillies[20], J. Goldberg[22], D.M. Gingrich[30,a], M.J. Goodrick[5], W. Gorn[4], C. Grandi[2], F.C. Grant[5], J. Hagemann[27], G.G. Hanson[12], M. Hansroul[8], C.K. Hargrove[7], P.F. Harrison[13], J. Hart[8], P.M. Hattersley[1], M. Hauschild[8], C.M. Hawkes[8], E. Heflin[4], R.J. Hemingway[6], G. Herten[10], R.D. Heuer[8], J.C. Hill[5], S.J. Hillier[8], T. Hilse[10], D.A. Hinshaw[18], J.D. Hobbs[8], P.R. Hobson[25], D. Hochman[26], R.J. Homer[1], A.K. Honma[28,a], R.E. Hughes-Jones[16], R. Humbert[10], P. Igo-Kemenes[11], H. Ihssen[11], D.C. Imrie[25], A.C. Janissen[6], A. Jawahery[17], P.W. Jeffreys[20], H. Jeremie[18], M. Jimack[1], M. Jones[29], R.W.L. Jones[8], P. Jovanovic[1], C. Jui[4], D. Karlen[6], K. Kawagoe[24], T. Kawamoto[24], R.K. Keeler[28], R.G. Kellogg[17], B.W. Kennedy[15], J. King[13], S. Kluth[5], T. Kobayashi[24], D.S. Koetke[8], T.P. Kokott[3], S. Komamiya[24], J.F. Kral[8], R. Kowalewski[8], J. von Krogh[11], J. Kroll[9], P. Kyberd[13], G.D. Lafferty[16], H. Lafoux[21], R. Lahmann[17], J. Lauber[8], J.G. Layter[4], P. Leblanc[18], A.M. Lee[31], E. Lefebvre[18], M.H. Lehto[15], D. Lellouch[26], C. Leroy[18], J. Letts[4], L. Levinson[26], S.L. Lloyd[13], F.K. Loebinger[16], J.M. Lorah[17], B. Lorazo[18], M.J. Losty[7], X.C. Lou[12], J. Ludwig[10], A. Luig[10], M. Mannelli[8], S. Marcellini[2], C. Markus[3], A.J. Martin[13], J.P. Martin[18], T. Mashimo[24], P. Mättig[3], U. Maur[3], J. McKenna[29], T.J. McMahon[1], J.R. McNutt[25], F. Meijers[8], D. Menszner[11], F.S. Merritt[9], H. Mes[7], A. Michelini[8], R.P. Middleton[20], G. Mikenberg[26], J. Mildenberger[6], D.J. Miller[15], R. Mir[12], W. Mohr[10], C. Moisan[18], A. Montanari[2], T. Mori[24], M. Morii[24], U. Müller[3], B. Nellen[3], H.H. Nguyen[9], S.W. O'Neale[1], F.G. Oakham[7], F. Odorici[2], H.O. Ogren[12], C.J. Oram[28,a], M.J. Oreglia[9], S. Orito[24], J.P. Pansart[21], B. Panzer-Steindel[8], P. Paschievici[26], G.N. Patrick[20], N. Paz-Jaoshvili[23], M.J. Pearce[1], P. Pfister[10], J.E. Pilcher[9], J. Pinfold[30], D. Pitman[28], D.E. Plane[8], P. Poffenberger[28], B. Poli[2], T.W. Pritchard[13], H. Przysiezniak[18], G. Quast[27], M.W. Redmond[8], D.L. Rees[8], G.E. Richards[16], M. Rison[5], S.A. Robins[5], D. Robinson[8], A. Rollnik[3], J.M. Roney[28], E. Ros[8], S. Rossberg[10], A.M. Rossi[2], M. Rosvick[28], P. Routenburg[30], K. Runge[10], O. Runolfsson[8], D.R. Rust[12], M. Sasaki[24], C. Sbarra[2], A.D. Schaile[26], O. Schaile[10], W. Schappert[6], F. Scharf[3], P. Scharff-Hansen[8], P. Schenk[4], B. Schmitt[3], H. von der Schmitt[11], M. Schröder[12], C. Schwick[27], J. Schwiening[3], W.G. Scott[20], M. Settles[12], T.G. Shears[5], B.C. Shen[4], C.H. Shepherd-Themistocleous[7], P. Sherwood[15], G.P. Siroli[2], A. Skillman[16], A. Skuja[17], A.M. Smith[8], T.J. Smith[28], G.A. Snow[17], R. Sobie[28], R.W. Springer[17], M. Sproston[20], A. Stahl[3], C. Stegmann[10], K. Stephens[16], J. Steuerer[28], R. Ströhmer[11], D. Strom[19], H. Takeda[24], T. Takeshita[24,c], S. Tarem[26], M. Tecchio[9], P. Teixeira-Dias[11], N. Tesch[3], M.A. Thomson[15], E. Torrente-Lujan[22], S. Towers[28], G. Transtromer[25], N.J. Tresilian[16], T. Tsukamoto[24], M.F. Turner[8], D. Van den plas[18], R. Van Kooten[27], G.J. VanDalen[4], G. Vasseur[21], A. Wagner[27], D.L. Wagner[9], C. Wahl[10], C.P. Ward[5], D.R. Ward[5], P.M. Watkins[1], A.T. Watson[1], N.K. Watson[8], M. Weber[11], P. Weber[6], P.S. Wells[8], N. Wermes[3], M.A. Whalley[1], B. Wilkens[10], G.W. Wilson[4], J.A. Wilson[1], V-H. Winterer[10], T. Wlodek[26], G. Wolf[26], S. Wotton[11], T.R. Wyatt[16], R. Yaari[26], A. Yeaman[13], G. Yekutieli[26], M. Yurko[18], W. Zeuner[8], G.T. Zorn[17].

[1]School of Physics and Space Research, University of Birmingham, Birmingham, B15 2TT, UK
[2]Dipartimento di Fisica dell' Università di Bologna and INFN, Bologna, 40126, Italy
[3]Physikalisches Institut, Universität Bonn, D-5300 Bonn 1, Germany
[4]Department of Physics, University of California, Riverside, CA 92521 USA
[5]Cavendish Laboratory, Cambridge, CB3 0HE, UK
[6]Carleton University, Dept of Physics, Colonel By Drive, Ottawa, Ontario K1S 5B6, Canada
[7]Centre for Research in Particle Physics, Carleton University, Ottawa, Ontario K1S 5B6, Canada
[8]CERN, European Organisation for Particle Physics, 1211 Geneva 23, Switzerland
[9]Enrico Fermi Institute and Dept of Physics, University of Chicago, Chicago Illinois 60637, USA
[10]Fakultät für Physik, Albert Ludwigs Universität, D-7800 Freiburg, Germany
[11]Physikalisches Institut, Universität Heidelberg, Heidelberg, Germany
[12]Indiana University, Dept of Physics, Swain Hall West 117, Bloomington, Indiana 47405, USA
[13]Queen Mary and Westfield College, University of London, London, E1 4NS, UK
[14]Birkbeck College, London, WC1E 7HV, UK
[15]University College London, London, WC1E 6BT, UK
[16]Department of Physics, Schuster Laboratory, The University, Manchester, M13 9PL, UK
[17]Department of Physics, University of Maryland, College Park, Maryland 20742, USA
[18]Laboratoire de Physique Nucléaire, Université de Montréal, Montréal, Quebec, H3C 3J7, Canada
[19]University of Oregon, Dept of Physics, Eugene, Oregon 97403, USA
[20]Rutherford Appleton Laboratory, Chilton, Didcot, Oxfordshire, OX11 0QX, UK
[21]DAPNIA/SPP, Saclay, F-91191 Gif-sur-Yvette, France
[22]Department of Physics, Technion-Israel Institute of Technology, Haifa 32000, Israel
[23]Department of Physics and Astronomy, Tel Aviv University, Tel Aviv 69978, Israel
[24]International Centre for Elementary Particle Physics and Dept of Physics, University of Tokyo, Tokyo 113, and Kobe University, Kobe 657, Japan
[25]Brunel University, Uxbridge, Middlesex, UB8 3PH UK
[26]Nuclear Physics Department, Weizmann Institute of Science, Rehovot, 76100, Israel
[27]Universität Hamburg/DESY, II Inst für Experimental Physik, Notkestrasse 85, 22607 Hamburg, Germany
[28]University of Victoria, Dept of Physics, P O Box 3055, Victoria BC V8W 3P6, Canada
[29]University of British Columbia, Dept of Physics, Vancouver BC V6T 1Z1, Canada
[30]University of Alberta, Dept of Physics, Edmonton AB T6G 2N5, Canada
[31]Duke University, Dept of Physics, Durham, North Carolina 27708-0305, USA

[a]Also at TRIUMF, Vancouver, Canada V6T 2A3
[b]Now at MPI, München, Germany
[c]Also at Shinshu University, Matsumoto 390, Japan

1 Introduction

A precise measurement of the partial width for the decay $Z^0 \to b\bar{b}$ would provide a stringent test of the Standard Model [1] and some possible extensions [2]. Measurements that have been performed to date make use of semi-leptonic b quark decays [3, 4, 5] and impact parameter distributions of tracks from b-flavoured hadron decay [6, 7]. Differences in event shapes between $Z^0 \to b\bar{b}$ and Z^0 decays into other quarks [8] can also be used, although the accuracy of this technique is limited by uncertainties in the modelling of hadronisation. The Z^0 partial decay width into b quarks, $\Gamma_{b\bar{b}}$, is measured by selecting hadronic Z^0 decays and determining the fraction of decays into $b\bar{b}$ pairs in the selected sample, $\Gamma_{b\bar{b}}/\Gamma_{had} \equiv \Gamma(Z^0 \to b\bar{b})/\Gamma(Z^0 \to \text{hadrons})$. This paper describes a new method of measuring the fraction of Z^0 decays into $b\bar{b}$ pairs in the hadronic event sample.

In the "mixed tag" method each event is divided into two hemispheres by the plane perpendicular to the thrust axis. The presence of a b quark in a hemisphere is tagged by either a high momentum lepton or several tracks with a large impact parameter. The fractions of hemispheres with a lepton or impact parameter tag are measured, as are the fractions of events with combinations of these tags in opposite hemispheres. The expected tagging fractions can be expressed in terms of the efficiencies of tagging individual quark flavours and the partial widths of the Z^0 decaying into these flavours. The resulting expressions are used to derive $\Gamma_{b\bar{b}}/\Gamma_{had}$, the efficiencies of correctly identifying b quark hemispheres for both tagging techniques, and the impact parameter tagging efficiency for background. This procedure renders the result for $\Gamma_{b\bar{b}}/\Gamma_{had}$ insensitive to branching fractions, fragmentation and decay modelling for b quarks and b-flavoured hadrons. It also allows the use of impact parameter tags that are relatively impure, but have high efficiency.

The following sections describe the OPAL detector, the selection of hadronic Z^0 decays, the two tagging techniques for hemispheres containing a b quark, and the application of the mixed tag method to measure $\Gamma_{b\bar{b}}/\Gamma_{had}$. These are followed by the presentation of the result and a detailed investigation of possible systematic effects.

2 The OPAL detector

The OPAL detector has been described in detail elsewhere [9, 10]. Only a brief account of some relevant features for the present analysis is given here.

The tracking of charged particles is performed with a central detector that contains three systems of drift chambers: a precision inner vertex chamber, a large volume jet chamber and specialised chambers at the outer radius of the jet chamber which improve track position measurements in the z-direction.[1] The tracking chambers are enclosed by a solenoidal magnet coil providing an axial field of 0.435 T. The average angular resolution of the combined tracking system is about 0.2 mrad in ϕ and better than 10 mrad in θ. The OPAL central detector also includes a silicon microvertex detector (μVTX) [10], installed during the 1990-1991 LEP shutdown. This device consists of two layers of silicon microstrip detectors positioned close to the e^+e^- collision point, one at a radius of 6.1 cm with an angular coverage of $|\cos\theta| < 0.83$, and one at a radius of 7.5 cm with a coverage of $|\cos\theta| < 0.77$. For tracks that are reconstructed in hadronic Z^0 decays in the other tracking chambers and that pass through the active silicon region, a positional resolution of about 9 μm and an efficiency of about 95% for finding at least one silicon detector hit on a track is presently achieved with this detector. For 45 GeV/c muons, the impact parameter resolution in the r-ϕ plane is 18 μm when there are μVTX hits on the track and 42 μm otherwise.

Electromagnetic energy is measured by a detector composed of lead-glass blocks located outside the magnet coil, divided into a barrel ($|\cos\theta| < 0.82$) and two endcaps ($0.81 < |\cos\theta| < 0.98$). Each block subtends approximately 40×40 mrad^2. The depth of material to the back of the calorimeter

[1] The coordinate system is defined so that z is the coordinate parallel to the e^+ and e^- beam axis, r is the coordinate normal to the beam axis, ϕ is the azimuthal angle and θ is the polar angle with respect to the z-axis.

is about 25 radiation lengths. The electromagnetic calorimeter has a presampler in front of it, which consists of limited streamer tubes in the barrel region and thin multiwire chambers for the endcaps. This presampler provides discrimination between electromagnetic and hadronic shower profiles.

Outside the electromagnetic calorimeter, the OPAL detector is instrumented with a hadron calorimeter, constructed from alternating layers of iron slabs and limited streamer tubes. The thickness of the material is typically eight interaction lengths. Outside the hadron calorimeter is the muon chamber system, comprised of four layers of drift chambers for $|\cos\theta| < 0.68$ and four layers of limited streamer tubes for $0.60 < |\cos\theta| < 0.98$. The typical position resolution of the muon chambers is about 2 mm.

3 Event selection

The OPAL trigger and online event selection systems are described in [11] and [12] respectively. Hadronic events are selected offline by imposing the same requirements used to measure the hadronic width of the Z^0 [13]. Within the geometrical region used for the present study, the efficiency of this selection is greater than 99.6%.

Tracks and electromagnetic calorimeter clusters used in the analysis are required to pass quality cuts. Charged tracks are required to have at least 20 measured points in the jet chamber, to have a transverse momentum in the r-ϕ plane greater than 0.15 GeV/c, to lie in the region $|\cos\theta| < 0.94$ and to pass within 5 cm in the r-ϕ plane and 200 cm along the z-axis from the origin at the point of closest approach in the r-ϕ plane. In addition, they are required to have a χ^2 per degree-of-freedom of less than 100 for the track fit in the r-ϕ plane and to have a reconstructed momentum of less than 65 GeV/c. Events are accepted only if they have seven or more charged tracks passing these criteria. The analysis uses reconstructed clusters of energy, i.e. groups of contiguous lead glass blocks which contain at least 0.1 GeV if they are in the barrel region or contain at least 0.2 GeV and consist of at least two lead glass blocks if they are in the endcap region. A cluster is associated with a charged track if the extrapolated track coordinates at the entrance of the calorimeter match the cluster centroid position to within 80 mrad in ϕ and 150 mrad in θ if the cluster is in the barrel, or 50 mrad in both ϕ and θ if it is in the endcap.

The analysis uses samples of hadronic events collected in 1990 and 1991. These events were produced at centre-of-mass energies ranging between 88.2 GeV and 94.2 GeV. Most of the integrated luminosity was acquired at the Z^0 peak and the distribution of the events over this range of energies has a negligible effect on the fraction of $b\bar{b}$ events in the sample. The 1991 data sample is divided into those events for which the μVTX was not yet operational and those for which μVTX information is added to the track fits. A total of 139 452, 91 370 and 241 526 hadronic Z^0 decays are obtained for further analysis in the 1990, 1991 without μVTX, and 1991 with μVTX data samples, corresponding to a total integrated luminosity of 21 pb^{-1}.

All track parameters are evaluated with respect to the primary event vertex. The primary vertex is fitted separately in each event and the average beam spot position [14] is used as a constraint. The beam spot size is determined to be 150 μm in the x and 8 μm in the y direction. The resolution on the fitted primary vertex is typically 60 μm along the x-axis and 10 μm along the y-axis.

Tracks are clustered into jets using the JADE jet-finding algorithm [15]. Charged tracks and unassociated electromagnetic energy clusters passing the selection criteria described above are used in the E0 scheme of the jet-finder. A minimum invariant mass squared threshold of $x_{\rm min} = 49$ (GeV/c^2)^2 is used.

Events are split into two hemispheres with the plane of division perpendicular to the thrust axis. The thrust value and axis are determined with the same charged tracks and unassociated clusters as for the jet-finding described above. The mixed tag method is sensitive to non-uniform tagging efficiencies that are correlated between the two hemispheres. To reduce kinematic correlations, e.g. due to hard gluon bremsstrahlung, only events with thrust value $T > 0.8$ are retained. Geometric correlations can be reduced significantly by considering only events with $|\cos\theta_{\rm thrust}| \leq 0.6$. The numbers of events

remaining after these requirements are respectively 67 294, 43 995 and 116 502 for the three data sets listed above.

4 Monte Carlo simulation

The data were simulated by the JETSET Monte Carlo event generator version 7.3 [16] and the full OPAL detector simulation package [17]. Heavy quarks were fragmented according to the formula of Peterson et al. [18], with mean momentum fraction divided by beam energy $\langle x_E \rangle_c = 0.51$ (corresponding to $\epsilon_c = 0.05$) for charmed hadrons and $\langle x_E \rangle_b = 0.70$ (corresponding to $\epsilon_b = 0.0055$) for b-flavoured hadrons [19, 5]. The momentum spectrum of leptons from semi-leptonic decays of charmed flavoured hadrons was modelled with the ACCMM model tuned to DELCO data [20]. The branching ratio $Br(c \to \ell)$ was taken to be $(9.6 \pm 1.1)\%$ [4, 21]. The average b-flavoured hadron lifetime was set to $\langle \tau_B \rangle = 1.4$ ps. Data and Monte Carlo events were processed through the same reconstruction and analysis programs. To obtain better agreement between Monte Carlo and data, reconstructed track parameters were degraded by 40% to 50% in the Monte Carlo. For the relevant distributions, like that of the impact parameter, good agreement is obtained after this additional smearing.

5 Identification of $Z^0 \to b\bar{b}$ events

The mixed tag method makes use of two independent identification methods. The tagging techniques considered are described below.

5.1 Identifying b-flavoured hadron decays with leptons

The semi-leptonic decay of b-flavoured hadrons results in a lepton with large momentum, p, and transverse momentum, p_t, with respect to the jet containing the lepton,[2] because of the hard fragmentation and the high mass of b quarks compared to other quark flavours produced in Z^0 decays. Therefore, the presence of electrons or muons with large p and p_t allows the separation of a sample of $b\bar{b}$ events with high purity [4].

For the purpose of b quark identification, a hemisphere tagged by either an electron or a muon will be counted as a lepton tag. For the calculation of background, hemispheres that contain both a tagged electron and muon are arbitrarily considered as being tagged by an electron. This means that the muon tag background is normalised to the total number of hemispheres minus the number of hemispheres tagged by an electron.

The selection procedure for electrons can be found in reference [4]. It is based on the specific energy loss, dE/dx, measured in the jet chamber, the pulse height of presampler clusters associated to the track, the agreement of track momentum and energy seen in the electromagnetic calorimeter, and the lateral spread of the electromagnetic shower. Tracks are accepted as electron candidates only if $|\cos\theta_{\rm track}| < 0.7$. This corresponds to a region of clean acceptance of the chambers that make a precise z-coordinate measurement. The presence of a b-flavoured hadron in a hemisphere is identified by the electron tag if at least one electron candidate is found with $p > 4.0$ GeV/c and $p_t > 0.8$ GeV/c in the hemisphere.

The selection procedure for muons can also be found in reference [4]. It relies on the precise matching of extrapolated central detector tracks with track segments in the muon chambers. Muon candidates are accepted for $|\cos\theta| < 0.95$. The presence of a b-flavoured hadron in a hemisphere is identified by the muon tag if at least one muon candidate track is found with $p > 4.0$ GeV/c and $p_t > 1.0$ GeV/c in the hemisphere. With these kinematic cuts the electron and muon background uncertainties are approximately the same.

[2] The lepton is included in the jet axis calculation.

5.2 Identifying b-flavoured hadron decays using impact parameter information

The absolute value of the impact parameter, b, is defined as the distance of closest approach between the track and the primary event vertex position in the plane perpendicular to the beam axis. The impact parameter is attributed a positive sign if the track crosses its containing jet axis downstream of the primary vertex position, otherwise it is negative. Using the jet direction to estimate the direction of the b-flavoured hadron, tracks originating from a vertex due to b quark decay will typically have a positive b. Negative b values for b quark decays can arise from signing errors due to a poor estimate of the b-flavoured hadron direction or due to tracking resolution. Tracks coming from the primary vertex will have positive and negative impact parameters with equal probability due to detector resolution.

The effective separation of a track from the primary vertex is better determined if the signed impact parameter of a track is normalised to its resolution. The impact parameter resolution, σ_b, takes into account tracking uncertainties as well as the uncertainty associated with the primary vertex position. The *significance*, S, is defined as the ratio:

$$S \equiv \frac{b}{\sigma_b} . \tag{1}$$

To suppress contributions from long-lived light hadrons, such as Λ's and K's, tracks with an impact parameter in the range $|b| \geq 3$ mm are rejected. This rejects about 15% of all selected tracks in a nearly flavour independent way. Tracks with $\sigma_b > 1$ mm, amounting to less than 1% of all selected tracks, are also rejected. Note that any flavour dependence of these cuts is absorbed in the tagging efficiencies, which are measured from the data, and therefore does not bias the result for $\Gamma_{b\bar{b}}/\Gamma_{had}$.

The presence of a b-flavoured hadron decay can be tagged by the *forward multiplicity* [6, 7], which simply counts the number of tracks, M, with significance above a given threshold. To apply the mixed tag method, the forward multiplicity is calculated for each hemisphere separately.

Figure 1 shows the forward multiplicity distribution for $S \geq 3$ for the 1991 data including μVTX information. There is reasonable agreement between data and Monte Carlo. It will be shown that this analysis is not particularly sensitive to the detailed agreement of data and Monte Carlo events for the forward multiplicity.

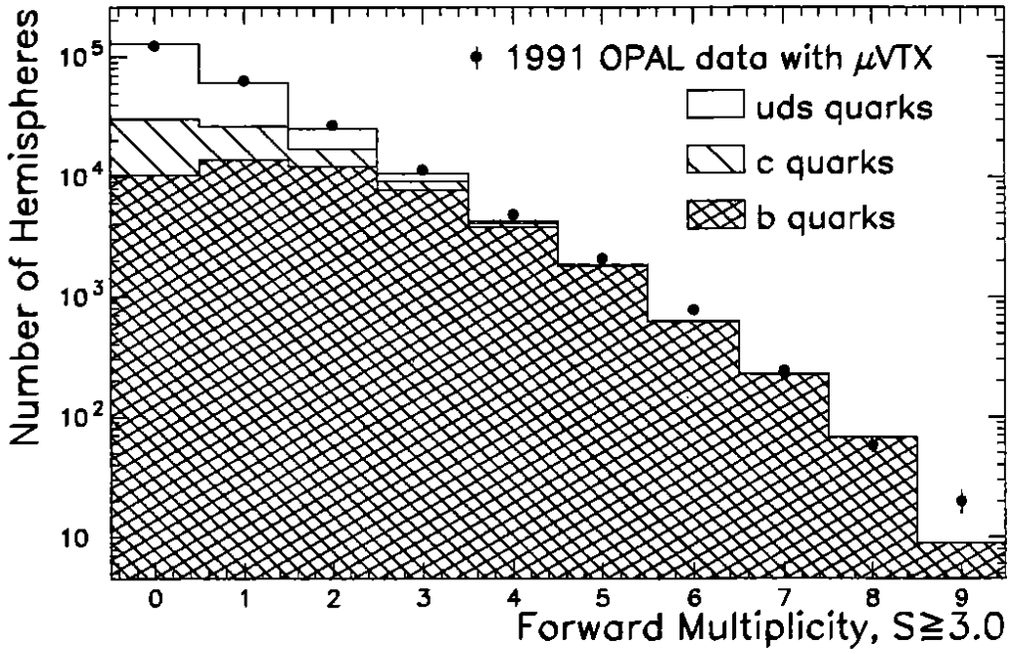

Figure 1: The forward multiplicity distribution with significance $S \geq 3$ for the 1991 data with μVTX information (full dots). The histogram indicates the Monte Carlo prediction.

The presence of a b-flavoured hadron in a hemisphere is identified by the forward multiplicity tag if at least $M^{\min} = 2$ tracks are found in the hemisphere with significance greater than or equal to $S^{\min} = 3$.

6 The mixed tag method to measure $\Gamma_{b\bar{b}}/\Gamma_{had}$

Using the impact parameter and lepton tags, the occurrence of five tagging topologies can be counted:

N_t the number of hemispheres tagged by tag t, where t can be v for the impact parameter tag, or ℓ for the lepton tag. These single tags provide two different topologies.

$N_{t_1 t_2}$ the number of events with tag t_1 in one hemisphere and tag t_2 in the other hemisphere, where t_1 and t_2 can be either of the two tags mentioned above. When $t_1 = t_2 = t$ the event is called a "double t tag", and if $t_1 \neq t_2$ it is called a "$t_1 t_2$ mixed tag". For the mixed tag events, $N_{v\ell}$ is defined as the sum of the two possible permutations in the tag indices. There are two double tag topologies and one mixed tag topology.

Table 1 gives the observed number of counts for the different topologies.

tag topology	1990 data	1991 data no μVTX	1991 data with μVTX
N_v	20124	12205	46420
N_ℓ	2519	1607	4342
N_{vv}	2466	1389	8374
$N_{v\ell}$	857	497	2048
$N_{\ell\ell}$	69	48	143
$N_{\rm tot}$	67294	43995	116502

Table 1: The number of hemispheres tagged by forward multiplicity (N_v) or leptons (N_ℓ), and the number of events tagged in both hemispheres by a combination of these (N_{vv}, $N_{v\ell}$, $N_{\ell\ell}$). $N_{\rm tot}$ is the total number of hadronic Z^0 decays passing the event selection.

The number of counts for each topology is normalised by the total number of hadronic Z^0 decays passing the event selection, $N_{\rm tot}$, to obtain the tagging fractions. The expected values of these fractions can be expressed as sums of products of efficiencies and partial widths. For the single tags this provides two expressions ($t = v, \ell$):

$$\frac{N_t}{2N_{\rm tot}} = \epsilon_t^{\rm b}\frac{\Gamma_{b\bar{b}}}{\Gamma_{\rm had}} + \epsilon_t^{\rm c}\frac{\Gamma_{c\bar{c}}}{\Gamma_{\rm had}} + \epsilon_t^{\rm uds}\frac{\Gamma_{\rm uds}}{\Gamma_{\rm had}} \,. \tag{2}$$

Similarly, two equations give the double tag fractions:

$$\frac{N_{tt}}{N_{\rm tot}} = C_{tt}^{\rm b}(\epsilon_t^{\rm b})^2\frac{\Gamma_{b\bar{b}}}{\Gamma_{\rm had}} + C_{tt}^{\rm c}(\epsilon_t^{\rm c})^2\frac{\Gamma_{c\bar{c}}}{\Gamma_{\rm had}} + C_{tt}^{\rm uds}(\epsilon_t^{\rm uds})^2\frac{\Gamma_{\rm uds}}{\Gamma_{\rm had}} \,. \tag{3}$$

The mixed tag fraction is:

$$\frac{N_{v\ell}}{2N_{\rm tot}} = C_{v\ell}^{\rm b}\epsilon_v^{\rm b}\epsilon_\ell^{\rm b}\frac{\Gamma_{b\bar{b}}}{\Gamma_{\rm had}} + C_{v\ell}^{\rm c}\epsilon_v^{\rm c}\epsilon_\ell^{\rm c}\frac{\Gamma_{c\bar{c}}}{\Gamma_{\rm had}} + C_{v\ell}^{\rm uds}\epsilon_v^{\rm uds}\epsilon_\ell^{\rm uds}\frac{\Gamma_{\rm uds}}{\Gamma_{\rm had}} \,. \tag{4}$$

The symbols introduced are defined as follows:

ϵ_t^q	the efficiency of selecting a hemisphere with the tag method t for quark flavour q, where t can be v or ℓ, and q can be b, c or uds,
$C_{t_1 t_2}^q$	the correlation factor for the double or mixed tagging efficiencies in the opposite hemispheres of an event. As above, t_1 and t_2 can be v or ℓ. The absence of correlations corresponds to $C_{t_1 t_2}^q = 1$.
$\Gamma_{b\bar{b}}/\Gamma_{had}$	the fraction of hadronic Z^0 decays into b quarks,
$\Gamma_{c\bar{c}}/\Gamma_{had}$	the fraction of hadronic Z^0 decays into c quarks,
$\Gamma_{uds}/\Gamma_{had}$	the fraction of hadronic Z^0 decays into u, d, and s quarks. Note that $\Gamma_{uds}/\Gamma_{had}$ is taken to be $1 - \Gamma_{b\bar{b}}/\Gamma_{had} - \Gamma_{c\bar{c}}/\Gamma_{had}$.

$\Gamma_{b\bar{b}}/\Gamma_{had}$, ϵ_v^b, ϵ_ℓ^b and ϵ_v^c are derived from the data using these relations as described in section 7 below. The parameter ϵ_v^{uds} is taken to be related to ϵ_v^c through

$$\epsilon_v^{uds} = \kappa \epsilon_v^c \ , \tag{5}$$

where the parameter κ is determined from Monte Carlo studies. The parameters ϵ_ℓ^c and ϵ_ℓ^{uds} are obtained from an analysis of the backgrounds to the lepton tagged sample. The correlation factors are studied using the Monte Carlo and the data. The value of C_{vv}^b predicted by the Monte Carlo is used in the analysis. All other correlation factors are taken to be unity. Systematic effects on the value of C_{vv}^b as determined from Monte Carlo simulation are discussed later, as well as cross checks on this and other efficiency correlations between hemispheres from the data. The Z^0 decay width into charm quarks, $\Gamma_{c\bar{c}}/\Gamma_{had}$, is taken as the Standard Model prediction [22]:

$$\frac{\Gamma_{c\bar{c}}}{\Gamma_{had}} = 0.171 \ . \tag{6}$$

An uncertainty of 22% on $\Gamma_{c\bar{c}}/\Gamma_{had}$ is taken, according to the published OPAL measurement [23].

6.1 Evaluation of κ

The ratio κ is obtained from a Monte Carlo study of the number of u, d and s quark hemispheres relative to the number of c quark hemispheres selected by the forward multiplicity tag. This ratio is estimated by:

$$\kappa = \frac{N_v^{uds}/(2N_{tot}^{uds})}{N_v^c/(2N_{tot}^c)} \ , \tag{7}$$

where N_v^{uds} is the number of hemispheres tagged by forward multiplicity for u, d and s quark events and N_{tot}^{uds} is the total number of u, d and s events. The numbers N_v^c and N_{tot}^c are defined analogously for c quarks. Table 2 presents the values of κ that were determined from Monte Carlo simulation.

There are two main sources of systematic uncertainty on the value of κ. There is a systematic error resulting from modelling of the detector resolution and a systematic error due to uncertainties in the modelling of the physics in the event generator. The systematic errors on κ are listed in Table 2.

The systematic uncertainty from detector resolution effects has been assessed by varying the smearing of the track impact parameter, azimuthal angle and curvature resolutions by $\pm 20\%$ with respect to the case of best agreement of Monte Carlo with data. With the 20% narrower or wider Monte Carlo distributions the disagreement with the data is rather distinct.

The lifetime of $D^\pm$ mesons is comparable to that of b-flavoured hadrons and is considerably longer than that for D^0 mesons. To account for the uncertainty in the size of the $D^\pm$ component in the charm background the fraction of $D^\pm$ mesons relative to D^0 mesons in $Z^0 \to c\bar{c}$ decays was taken to be $(46 \pm 20)\%$, where the error is a conservative estimate. The change in the average charmed hadron lifetime in $Z^0 \to c\bar{c}$ decays induced by this variation is large compared to uncertainties associated with the measured D meson lifetimes. The Peterson parameter for c quark fragmentation was also varied in the Monte Carlo simulation to give a mean x_E varying between 0.49 and 0.53 [19]. It was verified

	1990+1991 data no μVTX	1991 data with μVTX
κ	0.610	0.413
	$\sigma(\kappa)$	
Monte Carlo detector resolution	$^{+0.064}_{-0.047}$	$^{+0.090}_{-0.020}$
Peterson fragmentation $\Delta\langle x_E\rangle_c = \pm 0.02$	$^{+0.020}_{-0.018}$	$^{+0.003}_{-0.001}$
$D^{\pm}$ fraction	± 0.002	± 0.002
K^0 and hyperon production	± 0.029	± 0.020
Monte Carlo statistics	± 0.010	± 0.006
total	$^{+0.074}_{-0.059}$	$^{+0.092}_{-0.029}$

Table 2: Monte Carlo predicted ratio κ: the forward multiplicity tagging efficiency for u, d and s quark hemispheres divided by that for c quark hemispheres.

that varying the mean charm charged decay multiplicity by one unit gives a negligible change in κ, while this decay multiplicity is known to 0.15 units [24]. A change of half a unit in mean multiplicity for all events [25] is expected to give even smaller deviations, due to the cancellation in the ratio κ. The effect of the uncertainty in the K^0 production rate was tested by varying it by 7.1% [26]. The hyperon production rate was varied by a conservative 20%. These two variations give a corresponding uncertainty in κ of 3.2% and 3.5%.

The κ values for 1990 and 1991 data without μVTX agree within their statistical uncertainties and have been combined into one number.

The uncertainty on κ due to Monte Carlo statistics is added to the systematic error in quadrature.

6.2 Evaluation of the correlation factors

The correlation factors are estimated from a Monte Carlo study similar to that used to obtain κ. For the double tags, they are determined as:

$$C_{tt}^{q} = \frac{4N_{tt}^{q}N_{tot}^{q}}{(N_{t}^{q})^{2}} , \tag{8}$$

where t can be v or ℓ, and q can be b, c or uds. For the mixed tag, they are determined as:

$$C_{v\ell}^{q} = \frac{2N_{v\ell}^{q}N_{tot}^{q}}{N_{v}^{q}N_{\ell}^{q}} . \tag{9}$$

For the purity level of the tags considered here, the correlations for c events and u, d and s events have little impact on the result. The result is mainly sensitive to correlation factors departing from unity for the b events.

For $b\bar{b}$ events, the majority of the impact parameter tags come from tracks that originate from a decay vertex displaced from the primary event vertex. In these cases a displacement of the measured primary vertex position from the genuine primary vertex position can result in an anti-correlation of "apparent" lifetimes in the opposite hemispheres. The values for C_{vv}^{b} that are obtained from the Monte Carlo simulation are listed in Table 3.

	1990 data	1991 data no μVTX	1991 data with μVTX
C_{vv}^{b}	0.9694	0.9979	0.9849
	$\sigma(C_{vv}^{b})$		
Monte Carlo detector resolution	± 0.0180	$^{+0.0114}_{-0.0184}$	$^{+0.0020}_{-0.0005}$
Peterson fragmentation $\Delta\langle x_E\rangle_b = 0.02$	± 0.0021	± 0.0140	$^{+0.0012}_{-0.0023}$
average b hadron lifetime $\Delta\langle\tau_B\rangle = \pm 0.15$ ps	± 0.0041	± 0.0003	± 0.0009
10 μm shift in average beam spot position	± 0.0048	± 0.0004	± 0.0015
Monte Carlo statistics	± 0.0147	± 0.0118	± 0.0030
total	± 0.0246	± 0.0247	± 0.0042

Table 3: The correlation factors C_{vv}^{b}.

The systematic uncertainty on the Monte Carlo determination of C_{vv}^{b} is found by varying the impact parameter resolution by $\pm 20\%$, and conservatively changing the Peterson fragmentation parameter to vary $\langle x_E\rangle_b$ between 0.68 and 0.72 [19, 5]. The average b-flavoured hadron lifetime is varied by 0.15 ps in the Monte Carlo simulation, which is the difference between the value used in this analysis and a recent result, $\langle\tau_B\rangle = 1.523 \pm 0.051$ ps, published by OPAL [27]. In addition the effect of a systematic offset of 10 μm in the average beam spot position in both transverse directions was investigated. The Monte Carlo statistical error is also added as systematic uncertainty on C_{vv}^{b}. The results for the systematic errors on C_{vv}^{b} are listed in Table 3. Within the uncertainties, the values of C_{vv}^{b} for the 1990 and 1991 data without μVTX agree. However, because these values are not expected to agree perfectly due to differences in multiple scattering and small differences in the beam spot size between the data sets, they are treated separately.

The other correlation factors are taken to be unity. Possible remaining systematic effects will be discussed later.

6.3 Estimation of lepton background

In the kinematic region under consideration lepton production is dominated by the semi-leptonic decay of b-flavoured hadrons. The tagging probabilities for light and charm quarks can be expressed as:

$$\epsilon_\ell^{uds} = \frac{N_\ell^{uds}}{2N_{tot}^{uds}}, \tag{10}$$

$$\epsilon_\ell^{c} = \frac{N_{prompt}^{c}}{2N_{tot}^{c}} + \frac{N_{non-prompt}^{c}}{2N_{tot}^{c}} \tag{11}$$

respectively, where N_ℓ^{uds} is the number of lepton tags from u, d and s quarks from Z^0 decays, and N_{prompt}^{c} and $N_{non-prompt}^{c}$ are the numbers of prompt and non-prompt lepton tags from c quarks from Z^0 decays. N_{prompt}^{c} is defined to be the number of lepton tags from primary $c \to \ell$ decays. The other lepton tags, not coming from decays of primary c or b quarks, are called "non-prompt". Table 4 indicates the lepton background estimates discussed below. The numbers in the table were derived using $\Gamma_{c\bar{c}}/\Gamma_{had} = 0.171$ and $\Gamma_{b\bar{b}}/\Gamma_{had} = 0.218$. In the fit only tagging efficiencies for background are used, which are independent of the fractional widths.

	1990 data	1991 data no μVTX	1991 data with μVTX
N_e	1195	730	2020
N^c_{prompt}	133 ± 26	57 ± 11	151 ± 28
$N_\gamma + N_{Dalitz}$	80 ± 13	78 ± 13	138 ± 20
N_{misid}	93 ± 14	39 ± 4	107 ± 12
N_{decay}	4 ± 4	3 ± 3	8 ± 8
N_μ	1324	877	2322
N^c_{prompt}	80 ± 17	59 ± 12	157 ± 31
$N^c_{non-prompt}$	19 ± 5	11 ± 2	30 ± 6
N^{uds}_μ	68 ± 12	59 ± 8	156 ± 22

Table 4: Indication of the contribution of the electron and muon backgrounds to the total number of hemispheres tagged by a lepton. These numbers were derived using $\Gamma_{c\bar{c}}/\Gamma_{had} = 0.171$ and $\Gamma_{b\bar{b}}/\Gamma_{had} = 0.218$. In the fit only tagging efficiencies for background are used, which are independent of the fractional widths. The errors include the statistical and systematic uncertainties added in quadrature.

6.3.1 Prompt lepton background from primary c quarks

The number of hemispheres tagged by a prompt lepton produced in $Z^0 \to c\bar{c}$ events is obtained using the Monte Carlo simulation according to:

$$N^c_{prompt} = \left(N^c_{prompt}\right)^{MC} \left(\frac{\epsilon^{data}_{id}}{\epsilon^{MC}_{id}}\right) \left(\frac{N_{tot}}{N^{MC}_{tot}}\right) , \tag{12}$$

where $\left(N^c_{prompt}\right)^{MC}$ is the number of hemispheres tagged by prompt leptons from semi-leptonic charm quark decay as determined from the Monte Carlo.

A correction is applied for the difference in lepton identification efficiency between data, ϵ^{data}_{id}, and Monte Carlo, ϵ^{MC}_{id}, by multiplying by the ratio, $(\epsilon^{data}_{id}/\epsilon^{MC}_{id})$. For electrons this ratio is determined to be 1.19 ± 0.10 using the method described in [28] and is specific to prompt leptons from charm decay. For muons it is taken to be unity with an estimated uncertainty of 3.7% [4].

The background from semi-leptonic decay of charmed hadrons, as determined by the Monte Carlo simulation, inherits a systematic uncertainty of 11.5% from the above error on $Br(c \to \ell)$. A maximum variation in background of 5.2% for electrons and 7.5% for muons is found when the Peterson c quark fragmentation parameter is varied so as to vary $\langle x_E \rangle_c$ in the range $0.49 < \langle x_E \rangle_c < 0.53$.[19] In addition a semi-leptonic decay modelling uncertainty of 9% for the electrons and 12% for the muons is estimated from the difference between the ACCMM [20] model and the ISGW [29] model. These three sources of systematic errors are added in quadrature to give a 15.5% uncertainty on the number of electrons from charm decays and 18.2% on the number of muons from charm decays.

6.3.2 Non-prompt electron background

The non-prompt electron background is assumed to be independent of the primary quark flavour:

$$\frac{N_{non-prompt}}{2N_{tot}} = \frac{N^c_{non-prompt}}{2N^c_{tot}} = \frac{N^{uds}_\ell}{2N^{uds}_{tot}} \tag{13}$$

This assumption is supported by the Monte Carlo simulation that shows no flavour dependence for the non-prompt electron background. The yield of non-prompt electrons can be divided into four classes:

$$N_{non-prompt} = N_\gamma + N_{Dalitz} + N_{misid} + N_{decay} . \tag{14}$$

where

N_γ	is the number of hemispheres tagged by electrons originating from photon conversions,
$N_{\rm Dalitz}$	is the number of hemispheres tagged by electrons from Dalitz decays (i.e. $\pi^0, \eta \rightarrow e^+e^-\gamma$),
$N_{\rm misid}$	is the number of hemispheres tagged when hadrons are misidentified as electrons, and
$N_{\rm decay}$	is the number of hemispheres tagged by electrons from the weak decay of secondary hadrons, including c and b quarks produced in the fragmentation process.

An outline of the methods used to determine the background contributions is given below. The study of these sources of background is detailed in reference [4].

Tracks identified as electrons originating from photon conversions are identified, but not removed, using an algorithm explained in [4] with additional requirements to attain higher purity. The number of identified electrons from conversions is scaled to the total number of electrons from conversions using the efficiency and purity of the identified conversions sample as calculated from Monte Carlo simulations. The errors on the contribution from photon conversions come from data and Monte Carlo statistics and systematic errors arising from uncertainties in the Monte Carlo modelling of the data.

The Dalitz decay background is determined from Monte Carlo simulations. This is shown together with the conversion background in Table 4.

The number of hadrons misidentified as electrons is measured from the data as described in reference [4]. The hadronic background determined in this way is $(7.8 \pm 1.2)\%$ for the 1990 data and $(5.3 \pm 0.6)\%$ for the 1991 data.

The background from weak decays, including those from heavy quarks produced in the fragmentation process, is determined from Monte Carlo simulations. The systematic uncertainty on this small background is taken to be 100%.

6.3.3 Non-prompt muon background

The non-prompt muon background is determined from the Monte Carlo simulation using the fake probability per track method discussed in [4]. Sources of non-prompt muon tags are decays in flight of π's and K's, and fake tags caused by misidentified hadrons due to sailthrough, punchthrough or muon chamber track segments that are incorrectly associated to central detector tracks. The number of non-prompt muons is determined for each flavour, q, by:

$$\left(\frac{N^{\mu}_{\rm non-prompt}}{N_{\rm tot}}\right)^{\rm q} = \left(\frac{\left(N^{\mu}_{\rm non-prompt}\right)^{\rm MC}}{N^{\rm MC}_{\rm tot}}\right)^{\rm q} \left(\frac{N^{\rm data}_{\rm tracks}}{N^{\rm MC}_{\rm tracks}}\right) \left(\frac{N^{\rm MC}_{\rm tot}}{N_{\rm tot}}\right) , \qquad (15)$$

where $N^{\rm data}_{\rm tracks}$ and $N^{\rm MC}_{\rm tracks}$ are the numbers of tracks, in the data and the Monte Carlo simulation respectively, passing the standard track selection cuts as well as momentum cuts of $p > 4$ GeV/c and $p_t > 1$ GeV/c. The probability of a track being incorrectly identified as a prompt muon is predicted by the Monte Carlo to be practically independent of the primary quark flavour. The scale factor is found to be $(N^{\rm data}_{\rm tracks}/N^{\rm MC}_{\rm tracks})\,(N^{\rm MC}_{\rm tot}/N_{\rm tot}) = 1.08$. The systematic error on the non-prompt muon background is assessed to be 13% for these p and p_t cuts.

7 Determination of $\Gamma_{\rm b\bar{b}}/\Gamma_{\rm had}$

The parameters $\Gamma_{\rm b\bar{b}}/\Gamma_{\rm had}$, $\epsilon^{\rm b}_v$, $\epsilon^{\rm b}_\ell$ and $\epsilon^{\rm c}_v$ are obtained from the data using a χ^2 function that is defined in terms of the differences between the left and right hand sides of the five equations (2) to (4), divided by the statistical uncertainties on the measured observables. The number of hemisphere tags

is statistically correlated with the number of double and mixed tag events. This correlation is unfolded by constructing orthogonal tagging variables from the variables presented in equations (2) to (4).

The χ^2 is summed over the three different data sets, corresponding to 15 statistically independent terms. The parameters ϵ_v^b, ϵ_ℓ^b and ϵ_v^c are allowed to vary independently for each data set, while $\Gamma_{b\bar{b}}/\Gamma_{had}$ is forced to be the same for all three data sets. This yields a total of ten fit parameters.

The combined result for the 1990 and 1991 data samples is:

$$\frac{\Gamma_{b\bar{b}}}{\Gamma_{had}} = 0.218 \pm 0.006 \text{ (stat)} .$$

The χ^2 for the fit is 1.7 for five degrees of freedom. The results for $\Gamma_{b\bar{b}}/\Gamma_{had}$ for the three different data sets are: $0.213^{+0.014}_{-0.013}$ for 1990, $0.221^{+0.019}_{-0.017}$ for 1991 without μVTX information and 0.219 ± 0.008 for 1991 including μVTX data. The χ^2/d.o.f. values are 0.99/1, 0.02/1 and 0.47/1 for the three data sets respectively.

Table 5 presents the results for the identification efficiencies of the lepton and forward multiplicity tagging methods. The parameter ϵ_v^c should not be interpreted as the charm tagging efficiency by forward multiplicity, but as an average background efficiency with the relative weights for $Z^0 \to c\bar{c}$ and $Z^0 \to u\bar{u}, d\bar{d}, s\bar{s}$ events determined by κ. Note that the b tagging efficiencies are inclusive and contain factors for kinematic and particle identification efficiencies, semi-leptonic branching fractions, and a component for accidentally tagging b quarks.

data set	ϵ_ℓ^b%	π_ℓ%	ϵ_v^b%	ϵ_v^c%	π_v%
1990	7.0 ± 0.3	81	38.2 ± 0.6	12.8 ± 0.3	56
1991 no μVTX	7.1 ± 0.3	85	34.8 ± 0.6	11.1 ± 0.3	55
1991 with μVTX	7.3 ± 0.2	85	53.4 ± 0.6	19.6 ± 0.5	58

Table 5: Results for the fitted efficiencies (ϵ) and purities (π). The quoted uncertainties are statistical only.

As additional information the purities of the single hemisphere tagged samples are also given in Table 5. These purities are defined as:

$$\pi_t \equiv \frac{\epsilon_t^b \Gamma_{b\bar{b}}/\Gamma_{had}}{N_t/(2N_{tot})} . \tag{16}$$

8 Discussion of systematic effects

The estimated magnitude of the systematic effects considered are summarised in Table 6.

Uncertainties in the $c \to \ell$ branching ratio for the different types of charmed hadrons, the charm semi-leptonic decay modelling, the lepton identification efficiencies, the non-prompt lepton background, and the electron background from photon conversions and Dalitz decays only affect the uncertainty on $\Gamma_{b\bar{b}}/\Gamma_{had}$ through the error they induce in the lepton background estimate. The uncertainties in the charged D meson fraction produced in $Z^0 \to c\bar{c}$ decays and in the charm fragmentation affect $\Gamma_{b\bar{b}}/\Gamma_{had}$ mostly through the lepton background, but also contribute to the $\Gamma_{b\bar{b}}/\Gamma_{had}$ uncertainty through the determination of κ. The uncertainty on b fragmentation, the average b-flavoured hadron lifetime and the average beam spot position give rise to an uncertainty on $\Gamma_{b\bar{b}}/\Gamma_{had}$ through the induced uncertainty on C_{vv}^b. The tracking resolution modelling uncertainty in the Monte Carlo affects κ and C_{vv}^b and their contributions partially cancel. The error due to Monte Carlo statistics receives uncorrelated contributions from the lepton background, κ and C_{vv}^b estimates. In the following the uncertainties due to tagging efficiency correlations between the two hemispheres in an event, event selection, and $\Gamma_{c\bar{c}}/\Gamma_{had}$ are explained. Also several additional systematic tests are described.

contribution	σ_{syst}
$Br(c \to \ell)$ ($\pm 11.5\%$)	± 0.0027
$c \to \ell$ decay modelling (ACCMM$\leftrightarrow$ISGW)	± 0.0031
muon identification efficiency ($\pm 3.7\%$)	± 0.0006
electron identification efficiency ($\pm 8.4\%$)	± 0.0013
non-prompt muon background ($\pm 13\%$)	± 0.0030
non-prompt electron background ($\pm 18.5\%$)	± 0.0022
photon conversions and Dalitz decays ($\pm 15.5\%$)	± 0.0018
$D^{\pm}/D^0$ ratio ($\pm 43\%$)	± 0.0019
K^0 and hyperon production rate	± 0.0005
c quark fragmentation ($0.49 < \langle x_E \rangle_c < 0.53$)	± 0.0020
b quark fragmentation ($0.68 < \langle x_E \rangle_b < 0.72$)	± 0.0008
average beam spot position uncertainty (± 10 μm)	± 0.0005
average b-flavoured hadron lifetime (± 0.15 ps)	± 0.0004
Monte Carlo detector resolution ($\pm 20\%$)	± 0.0004
Monte Carlo statistics	± 0.0021
global tagging efficiency correlation tests	± 0.0020
event selection	± 0.0007
total systematic error excluding $\Gamma_{c\bar{c}}/\Gamma_{\text{had}}$	± 0.0073
$\Gamma_{c\bar{c}}/\Gamma_{\text{had}}$	± 0.0070
total systematic error	± 0.0101

Table 6: Contributions to the systematic uncertainty on $\Gamma_{b\bar{b}}/\Gamma_{\text{had}}$.

8.1 Test of systematic effects from κ

As a check of systematic effects on κ from possible discrepancies between data and Monte Carlo for large values of M, the analysis was repeated with a forward multiplicity cut of $2 \leq M \leq 4$. This led to a change in $\Gamma_{b\bar{b}}/\Gamma_{\text{had}}$ of 0.003 ± 0.003(stat). Hence there is no evidence for a systematic effect on $\Gamma_{b\bar{b}}/\Gamma_{\text{had}}$ due to an imperfect description of κ at high M.

8.2 Uncertainties coming from efficiency correlations

As a check on the assumptions for the double and mixed tag correlation factors, the double and mixed tags were dropped in turn from the fit. When the double lepton tags were excluded the result became $\Gamma_{b\bar{b}}/\Gamma_{\text{had}} = 0.218 \pm 0.008$. When only the single and double lepton tags are used $\Gamma_{b\bar{b}}/\Gamma_{\text{had}} = 0.218^{+0.015}_{-0.013}$. Ignoring the double vertex tag or the mixed tag gives the same result, because these cases do not introduce additional degrees of freedom compared to the case of single and double lepton tags only. None of these tests gave evidence for deviations of the correlation factors from the values determined from the Monte Carlo simulated data.

A general check on geometrical correlations was also made. The event sample was divided into bins in ϕ or θ. One value of $\Gamma_{b\bar{b}}/\Gamma_{\text{had}}$ is fitted to all bins, but the efficiencies are free to vary for each bin. For the electrons the tagging efficiency is found to be constant in ϕ, but for the muons there is a region at the top and bottom of the detector with significantly lower efficiency than other regions in ϕ. Binning in ϕ to isolate the low efficiency region for muons results in a deviation of 0.0008 on $\Gamma_{b\bar{b}}/\Gamma_{\text{had}}$. The same binning in ϕ also serves as an indicator for possible correlations due to the primary vertex position resolution, which is much better in the vertical than in the horizontal direction. Similarly, a systematic error of 0.0008 is assigned for possible trends in the efficiencies with $|\cos\theta_{\text{thrust}}|$. This is obtained by using three bins of equal width in $|\cos\theta_{\text{thrust}}|$ on the 1991 data set including μVTX

information. The limited double lepton tag statistics do not allow this test to be performed on the other data sets.

Hadronic Z^0 events with a three and more jet topology differ from those with a two jet topology by the presence of one or more hard gluons in the final state. Hard gluons affect the momentum distribution of b-flavoured hadron decay products. This may introduce kinematic correlations in the tagging efficiencies. The dependence of the $\Gamma_{b\bar{b}}/\Gamma_{had}$ result upon the number of jets found in each event was examined using the full data sample. The events were divided into three categories: events with two jets, events with three jets and events with four jets or more. The difference between the event weighted average value for these three classes and the fit that does not distinguish between different numbers of jets per event is 0.0017. Monte Carlo studies indicate that a difference between the fit that is binned in number of jets and the unbinned fit is due to correlations in the electron tagging efficiencies. These correlations arise mostly because of the dependence of electron identification efficiency on particle activity close to the electron candidate track. This was confirmed by repeating the test on jet multiplicity for muons and impact parameter tags alone. In this case, a negligible effect on $\Gamma_{b\bar{b}}/\Gamma_{had}$ was observed.

A possible correlation arising from a variation of the tagging efficiencies in time was investigated by examining the single tag rates for 24 separate periods of data taking. No variations larger than those expected from statistical fluctuations were observed.

Special tests were performed on the correlation factors of the double vertex tag equations. As discussed above, a reason for the possible deviation of the double impact parameter tag correlation factor for b quarks from unity is the resolution on the primary vertex position, causing an anti-correlation between the tagging efficiency of the two hemispheres. The magnitude of this uncertainty was estimated by comparing $\Gamma_{b\bar{b}}/\Gamma_{had}$ obtained using the "true" and fitted primary vertex position in the Monte Carlo generated data. A difference of 0.0009 was found. This discrepancy is already accounted for in the previous systematic error estimates for C^b_{vv} and the other tagging efficiency correlations and is not included as a separate systematic error.

In conclusion, combining the errors 0.0008, 0.0008 and 0.0017, a total systematic uncertainty of 0.0020 is assigned to the $\Gamma_{b\bar{b}}/\Gamma_{had}$ result due to possible deviations of the correlation factors from their assumed values. This uncertainty is added independently from the uncertainties that arises from the Monte Carlo determination of C^b_{vv}, because they are connected to global tests that involve all correlation factors at the same time.

8.3 Event selection and thrust cut dependence

The change in the $Z^0 \to b\bar{b}$ event fraction due to the event selection was found to be $(0.08 \pm 0.34)\%$ from the Monte Carlo simulation. A 0.3% systematic uncertainty on $\Gamma_{b\bar{b}}/\Gamma_{had}$ is taken to account for a possible bias in the event selection.

The thrust cut was varied between 0.5, i.e. no cut at all, and 0.85. The observed variations were at most of order 0.001 and compatible with the relative statistical uncertainties between the different points. No change in the obtained $\Gamma_{b\bar{b}}/\Gamma_{had}$ value was observed when the event sample was divided into three thrust bins. Therefore, no systematic uncertainty is assigned for possible biases due to the thrust cut.

8.4 Dependence on $\Gamma_{c\bar{c}}/\Gamma_{had}$

The error on $\Gamma_{b\bar{b}}/\Gamma_{had}$ due to the $\pm 22\%$ uncertainty on $\Gamma_{c\bar{c}}/\Gamma_{had}$ [23] is ∓ 0.0070. The relation between the mean value of $\Gamma_{b\bar{b}}/\Gamma_{had}$ and $\Gamma_{c\bar{c}}/\Gamma_{had}$ is linear within this range of uncertainty.

8.5 Tests using other impact parameter and vertex tag algorithms

Two tests were performed to assess a possible bias introduced by the lifetime tag algorithm employed.

For both a forward multiplicity cut at two or more and three or more tracks, the significance cut was varied between 1.5 and 4.5. This covers a large area in the efficiency versus purity plane. The results for $\Gamma_{b\bar{b}}/\Gamma_{had}$ for some of these cut values are listed in Table 7. They are all compatible within

lifetime tagging method	$\Gamma_{b\bar{b}}/\Gamma_{had}$	$\langle\epsilon_v^b\rangle$ %	$\langle\pi_v\rangle$ %	χ^2/d.o.f.
forward multiplicity:				
$M^{min} = 2$ and $S^{min} = 1.5$	0.214 ± 0.003	72	39	4.4/5
$M^{min} = 2$ and $S^{min} = 2.0$	0.215 ± 0.002	62	46	6.6/5
$M^{min} = 2$ and $S^{min} = 2.5$	0.217 ± 0.002	53	52	3.4/5
$M^{min} = 2$ and $S^{min} = 3.0$ (nominal point)	0.218	45	57	1.7/5
$M^{min} = 2$ and $S^{min} = 3.5$	0.217 ± 0.002	39	60	3.8/5
$M^{min} = 2$ and $S^{min} = 4.0$	0.216 ± 0.003	33	62	4.4/5
$M^{min} = 2$ and $S^{min} = 4.5$	0.217 ± 0.003	29	65	4.0/5
$M^{min} = 3$ and $S^{min} = 2.0$	0.220 ± 0.003	36	65	9.2/5
$M^{min} = 3$ and $S^{min} = 3.0$	0.220 ± 0.003	23	78	1.5/5
$M^{min} = 3$ and $S^{min} = 4.0$	0.215 ± 0.004	15	84	0.9/5
secondary vertex method:				
$S^{min} = 10.0$	0.221 ± 0.005	11	88	2.8/5

Table 7: Results for $\Gamma_{b\bar{b}}/\Gamma_{had}$ for different lifetime tagging methods. The errors represent the statistical uncertainty with respect to the nominal point. The efficiency and purity values are event weighted averages for the three data sets.

the relative statistical uncertainty with the $\Gamma_{b\bar{b}}/\Gamma_{had}$ result at the nominal forward multiplicity cut values. Note that the $\Gamma_{b\bar{b}}/\Gamma_{had}$ values obtained at small significance values, such as $S^{min} \geq 1.5$, are affected by larger systematic uncertainties from κ than those of the nominal point. Nevertheless, all results are compatible with the nominal point within the relative statistical errors only.

As a second test a secondary vertex finder was used to form a tag using decay length significance. In this case, the significance is defined as the distance between the primary and the secondary vertex candidate divided by the uncertainty on this distance. The vertex finder takes all tracks inside a jet and forms a common vertex. Subsequently tracks with the largest χ^2 contribution are dropped successively from the fit until only tracks contributing less than 4.0 to the χ^2 are left. The remaining tracks are used to fit the position of the candidate secondary vertex. If less than four tracks are left, the fit is deemed to have failed. The vertex finding method showed little variation in $\Gamma_{b\bar{b}}/\Gamma_{had}$ (± 0.003), when varying the decay length significance cut between 6.0 and 14.0. As a representative point, the $\Gamma_{b\bar{b}}/\Gamma_{had}$ value obtained for a decay length significance cut of 10.0 is $\Gamma_{b\bar{b}}/\Gamma_{had} = 0.221^{+0.011}_{-0.010}$.

None of the lifetime tag techniques presented above gave deviations beyond those expected from statistical fluctuations. Therefore no additional systematic uncertainty is assigned due to variations when using different lifetime taggers.

8.6 Electrons and muons as separate tags

The equations (2) to (4) can be generalised to the case in which the lepton tag is divided into a separate electron and muon tag. In that case three single hemisphere tagging fractions, three double and three mixed tag fractions are obtained.

When the electrons and muons are treated as independent tags a value for $\Gamma_{b\bar{b}}/\Gamma_{had}$ of 0.218 ± 0.006 is obtained with a χ^2 of 6 for 14 degrees of freedom. Taking only electrons as lepton tags leads to $\Gamma_{b\bar{b}}/\Gamma_{had} = 0.222 \pm 0.011$, while muons only result in $\Gamma_{b\bar{b}}/\Gamma_{had} = 0.213 \pm 0.009$, where the χ^2 values are 2.5 and 1.5 for five degrees of freedom respectively. Note that the weighted average of the results for the electron and muon tags separately is not expected to reproduce the combined result exactly,

because events in which one hemisphere is tagged by an electron and the other by a muon are not considered when electron and muon tags are treated separately.

9 Combination with previously published OPAL results

This measurement of $\Gamma_{b\bar{b}}/\Gamma_{had}$ can be combined, according to the method described in [30], with previously published OPAL measurements from single electrons and muons [4], and an impact parameter method [6]. Table 8 contains the relative uncertainties separated according to source for the four measurements that are combined. Except for the statistical errors, errors on the same line are taken to be fully correlated between the measurements. Full statistical correlation between the single lepton tag results and the mixed tag result is assumed for the leptons within the common kinematic region. This leads to correlation coefficients of 0.50 and 0.58 between the analysis presented here and the single electron and muon tag analysis respectively. Also full correlation is assumed between the impact parameter statistical error and the statistical error component coming from the impact parameter tags in the 1990 data in the mixed tag, giving a correlation coefficient of 0.36. The average and its errors are not very sensitive to the precise assumptions on the above mentioned correlations and do not vary outside the quoted precision for extreme assumptions of these statistical correlations. The error from $\Gamma_{c\bar{c}}/\Gamma_{had}$ is included in deriving the weights. The resulting average is:

$$\frac{\Gamma_{b\bar{b}}}{\Gamma_{had}} = 0.220 \pm 0.004\ (\text{stat}) \pm 0.006\ (\text{syst})\ ,$$

and a change of $\Delta\Gamma_{c\bar{c}}/\Gamma_{had} = \pm 22\%$ results in a change of $\Delta\Gamma_{b\bar{b}}/\Gamma_{had} = \mp 0.006$, where the dependence is linear in this range. The weight of each individual measurement in the average is given at the bottom of Table 8. When the errors due to $\Gamma_{c\bar{c}}/\Gamma_{had}$ are ignored, the combined result does not deviate from the above value outside the quoted precision. In this case the relative weights for the single electron, the single muon, the impact parameter and this measurement become 14% : 12% : 39% : 36%.

A recent OPAL measurement that involves the fitting of the single and double lepton p and p_T spectra gives $\Gamma_{b\bar{b}}/\Gamma_{had} = 0.222 \pm 0.011(\text{stat}) \pm 0.007(\text{syst})$ [5]. This measurement is compatible with the above average. It is not included in the average, because of the large statistical correlation with the measurement presented in this paper.

10 Conclusions

The value of $\Gamma_{b\bar{b}}/\Gamma_{had}$ as measured with the mixed tag method is:

$$\frac{\Gamma_{b\bar{b}}}{\Gamma_{had}} = 0.218 \pm 0.006\ (\text{stat}) \pm 0.007\ (\text{syst}) \pm 0.007\ (\Gamma_{c\bar{c}}/\Gamma_{had})\ ,$$

where the first systematic uncertainty is specific to this analysis and the second systematic error is due to uncertainties in the $Z^0 \to c\bar{c}$ partial width.

This measurement of $\Gamma_{b\bar{b}}/\Gamma_{had}$ can be combined with previous OPAL measurements giving:

$$\frac{\Gamma_{b\bar{b}}}{\Gamma_{had}} = 0.220 \pm 0.004\ (\text{stat}) \pm 0.006\ (\text{syst}) \pm 0.006\ (\Gamma_{c\bar{c}}/\Gamma_{had})\ ,$$

The dependence of $\Gamma_{b\bar{b}}/\Gamma_{had}$ on $\Gamma_{c\bar{c}}/\Gamma_{had}$ is described by the linear relation $\Delta\Gamma_{b\bar{b}}/\Gamma_{b\bar{b}} = -0.114\Delta\Gamma_{c\bar{c}}/\Gamma_{c\bar{c}}$ in the range $0.13 < \Gamma_{c\bar{c}}/\Gamma_{had} < 0.21$.

The measured $\Gamma_{b\bar{b}}/\Gamma_{had}$ value is in good agreement with the Standard Model prediction of $\Gamma_{b\bar{b}}/\Gamma_{had} = 0.217$ for $M_{Z^0} = 91.175\ \text{GeV}/c^2$, $M_{top} = 140\ \text{GeV}/c^2$, $M_{Higgs} = 300\ \text{GeV}/c^2$ and $\alpha_s(M^2_{Z^0}) = 0.12$ [22], and with previously published measurements [3, 4, 5, 6, 7, 8].

	analysis				
source	single electron[4]	single muon[4]	impact param.[6]	this analysis	combined
$\Gamma_{b\bar{b}}/\Gamma_{had}$	0.216	0.224	0.222	0.218	0.220
experimental statistical error	1.4%	1.4%	3.2%	2.9%	1.8%
Monte Carlo statistical error	1.1%	1.2%	–	0.9%	0.7%
efficiency correlation	–	–	–	0.9%	0.2%
event selection efficiency	0.4%	0.4%	–	–	0.1%
bias due to kinematic cuts	–	–	1.8%	–	0.7%
event selection bias	0.3%	0.3%	0.3%	0.3%	0.3%
photon conversions	0.9%	–	–	0.8%	0.3%
electron hadronic background	0.2%	–	–	1.3%	0.4%
muon hadronic background	–	1.7%	–	1.3%	0.7%
electron id. eff. for b decays	2.9%	–	–	–	0.4%
muon id. eff. for b decays	–	3.7%	–	–	0.8%
lepton id. eff. for background	–	–	–	0.7%	0.2%
electron radiation loss	0.8%	–	–	–	0.1%
θ determination	–	0.4%	–	–	0.1%
tracking resolution	–	–	0.5%	0.2%	0.2%
tracking non-Gaussian tail	–	–	0.5%	–	0.2%
average beam spot	–	–	0.2%	0.2%	0.1%
$Br(b \to \ell)$	4.0%	4.2%	–	–	1.5%
$Br(b \to c \to \ell)$	1.9%	1.0%	–	–	0.5%
$Br(b \to J/\psi \to \ell)$	0.5%	0.4%	–	–	0.2%
$Br(b \to \tau \to \ell)$	0.6%	0.4%	–	–	0.2%
b semi-leptonic decay model	0.5%	0.3%	–	–	0.1%
b fragmentation	1.4%	1.2%	0.5%	0.4%	0.8%
b-flavoured hadron lifetime	–	–	0.5%	0.2%	0.2%
b decay multiplicity	–	–	1.8%	–	0.7%
c fragmentation	0.8%	0.3%	0.5%	0.9%	0.6%
$Br(c \to \ell)$	0.8%	0.5%	–	1.2%	0.5%
c decay model	0.9%	0.5%	–	1.4%	0.6%
$f(D^{\pm}) : f(D^0) : f(D_s) : f(\Lambda_c^{\pm})$	0.5%	0.3%	0.9%	0.9%	0.7%
light flavour multiplicity	–	–	0.5%	–	0.2%
K^0 and hyperon production	–	–	–	0.2%	0.1%
event generator	–	–	1.8%	–	0.7%
b/c from fragmentation	0.5%	0.4%	–	–	0.2%
syst. error excl. $\Gamma_{c\bar{c}}/\Gamma_{had}$	6.0%	6.4%	3.5%	3.4%	2.9%
$\Gamma_{c\bar{c}}/\Gamma_{had}$	1.9%	1.2%	3.0%	3.2%	2.5%
total systematic error	6.3%	6.5%	4.7%	4.7%	3.8%
total error	6.5%	6.6%	5.6%	5.5%	4.2%
weight in average	15%	21%	38%	26%	

Table 8: The uncertainties in the $\Gamma_{b\bar{b}}/\Gamma_{had}$ analyses that are combined. Those entries to which a measurement is not sensitive are marked by '–'.

The uncertainty due to $\Gamma_{c\bar{c}}/\Gamma_{had}$ is expected to decrease significantly as improved measurements are made. For the purposes of Standard Model fits, the relation given between $\Gamma_{c\bar{c}}/\Gamma_{had}$ and $\Gamma_{b\bar{b}}/\Gamma_{had}$ allows the correlations to be included properly.

With an increase in statistics the selection criteria for lepton and vertex tags can be modified to give purer tagged samples. This will reduce the systematic uncertainty from charm production and decay. The use of only long decay lengths should decrease the uncertainty from correlated vertex tagging efficiencies in opposite hemispheres, because the uncertainty in the primary vertex position becomes relatively less important.

Acknowledgements

It is a pleasure to thank the SL Division for the efficient operation of the LEP accelerator, the precise information on the absolute energy, and their continuing close cooperation with our experimental group. In addition to the support staff at our own institutions we are pleased to acknowledge the
Department of Energy, USA,
National Science Foundation, USA,
Texas National Research Laboratory Commission, USA,
Science and Engineering Research Council, UK,
Natural Sciences and Engineering Research Council, Canada,
Fussefeld Foundation,
Israeli Ministry of Energy and Ministry of Science,
Minerva Gesellschaft,
Japanese Ministry of Education, Science and Culture (the Monbusho) and a grant under the Monbusho International Science Research Program,
German Israeli Bi-national Science Foundation (GIF),
Direction des Sciences de la Matière du Commissariat à l'Energie Atomique, France,
Bundesministerium für Forschung und Technologie, Germany,
National Research Council of Canada,
A.P. Sloan Foundation and Junta Nacional de Investigação Científica e Tecnológica, Portugal.

References

[1] A. Blondel, A. Djouadi and C. Verzegnassi, Phys. Lett. B293 (1992) 253;
J. Bernabéu, A. Pich and A. Santamaría, Nucl. Phys. B363 (1991) 326;
A. Djouadi, et al., Nucl. Phys. B349 (1991) 48;
B. W. Lynn and R. G. Stuart, Phys. Lett. B252 (1990) 676;
F. Boudjema, A. Djouadi and C. Verzegnassi, Phys. Lett. B238 (1990) 423;
W. Beenakker and W. Hollik, Z. Phys. C40 (1988) 141;
J. Bernabéu, A. Pich and A. Santamaría, Phys. Lett. B200 (1988) 569;
A. A. Akhundov, D. Yu. Bardin and T. Riemann, Nucl. Phys. B276 (1986) 1.

[2] R. Chivukula, S. Selipsky and E. Simmons, Phys. Rev. Lett. 69 (1992) 575;
J. Layssac, F. M. Renard and C. Verzegnassi, Phys. Lett. B287 (1992) 267;
F. M. Renard and C. Verzegnassi, Phys. Lett. B260 (1991) 225;
M. Boulware and D. Finell, Phys. Rev. D44 (1991) 2054;
E. Nardi and E. Roulet, Phys. Lett. B248 (1990) 139;
G. Girardi, W. Hollik and C. Verzegnassi, Phys. Lett. B240 (1990) 492;
P. Langacker and D. London, Phys. Rev. D38 (1988) 886.

[3] DELPHI Collab., P. Abreu et al., Z. Phys. C56 (1992) 47;
OPAL Collab., P. Acton et al., Z. Phys. C55 (1992) 191;
OPAL Collab., M. Z. Akrawy et al., Phys. Lett. B263 (1991) 311;
L3 Collab., B. Adeva et al., Phys. Lett. B261 (1991) 177;
ALEPH Collab., D. Decamp et al., Phys. Lett. 244B (1990) 551;
L3 Collab., B. Adeva et al., Phys. Lett. B241 (1990) 416;
MARKII Collab., J. F. Kral et al., Phys. Rev. Lett. 64 (1990) 1211.

[4] OPAL Collab., P. Acton et al., *Measurement of* $\Gamma(Z^0 \to b\bar{b})/\Gamma(Z^0 \to hadrons)$ *Using Leptons*, CERN-PPE/93-46, to be published in Z. Phys. C.

[5] OPAL Collab., P. Acton et al., *Measurements of* $B^0\bar{B}^0$ *mixing* $\Gamma(Z^0 \to b\bar{b})/\Gamma(Z^0 \to hadrons)$ *and semileptonic branching ratios for b-flavoured hadrons in hadronic* Z^0 *decays*, CERN-PPE/93-106, submitted to Z. Phys. C.

[6] OPAL Collab., P. Acton et al., *A Measurement of* $\Gamma(Z^0 \to b\bar{b})/\Gamma(Z^0 \to hadrons)$ *Using an Impact Parameter Technique*, CERN-PPE/93-79, submitted to Z. Phys. C.

[7] ALEPH Collab., D. Buskulic et al., *A Precise Measurement of* $\Gamma_{Z\to b\bar{b}}/\Gamma_{Z\to hadrons}$, CERN-PPE/93-108, submitted to Phys. Lett. B;
MARKII Collab., R. Jacobsen et al., Phys. Rev. Lett. 67 (1991) 3347.

[8] ALEPH Collab., D. Buskulic et al., *Measurement of the Ratio* $\Gamma_{b\bar{b}}/\Gamma_{had}$ *using Event Shape Variables*, CERN-PPE/93-113, submitted to Phys. Lett. B;
L3 Collab., O. Adriani et al., Phys. Lett. B307 (1993) 237;
DELPHI Collab., P. Abreu et al., Phys. Lett. B295 (1992) 383;
DELPHI Collab., P. Abreu et al., Phys. Lett. B281 (1992) 383.

[9] OPAL Collab., K. Ahmet et al., Nucl. Instr. and Meth. A305 (1991) 275.

[10] P. P. Allport et al., Nucl. Instr. and Meth. A324 (1993) 34.

[11] M. Arignon et al., Nucl. Instr. and Meth. A313 (1992) 103.

[12] D. G. Charlton, F. Meijers, T. J. Smith and P. S. Wells,
Nucl. Instr. and Meth. A325 (1993) 129.

[13] OPAL Collab., G. Alexander et al., Z. Phys. C52 (1991) 175.

[14] The average beam spot position was calculated as described in:
OPAL Collab., P. Acton et al., Phys. Lett. B274 (1992) 513.

[15] OPAL Collab., M. Z. Akrawy et al., Z. Phys. C49 (1991) 375;
JADE Collab., S. Bethke et al., Phys. Lett. B213 (1988) 235;
JADE Collab., W. Bartel et al., Z. Phys. C33 (1986) 23.

[16] T. Sjöstrand, Comp. Phys. Comm. 39 (1986) 373.
The parameters were tuned to OPAL data as described in:
OPAL Collab., M. Z. Akrawy et al., Z. Phys. C47 (1990) 505.

[17] J. Allison et al., Nucl. Instr. Meth. A317 (1992) 47.

[18] C. Peterson, D. Schlatter, I. Schmitt and P. Zerwas, Phys. Rev. D27 (1983) 105.

[19] Average and uncertainty on $\langle x_E \rangle_c$ and $\langle x_E \rangle_b$ derived from combining the following published data:
DELPHI Collab., P. Abreu et al., Z. Phys. C56 (1992) 47;
L3 Collab., B. Adeva et al., Phys. Lett. B271 (1991) 461;
ALEPH Collab., D. Decamp et al., Phys. Lett. B266 (1991) 218;
OPAL Collab., M. Z. Akrawy et al., Phys. Lett. B263 (1991) 311;
OPAL Collab., G. Alexander et al., Phys. Lett. B262 (1991) 341;
ALEPH Collab., D. Decamp et al., Phys. Lett. B244 (1990) 551.

[20] G. Altarelli et al., Nucl. Phys. B264 (1991) 219.
The parameters of this model were taken to be $p_F = 282$ MeV/c and $m_s = 50$ MeV/c^2 from a fit described in:
CLEO Collab., S. Henderson et al., Phys. Rev. D45 (1992) 2212;
M. Worris, CLNS Thesis 91-05, Cornell University, 1991,
to DELCO data:
DELCO Collab., W. Bacino et al., Phys. Rev. Lett. 43 (1979) 1073.

[21] Particle Data Group, K. Hikasa et al., Phys. Rev. D45 (1992) 1.

[22] Standard Model prediction from ${}_{ZF}I^{T}T_{E_R}$ for $M_{Z^0} = 91.175$ GeV/c^2, $M_{\rm top} = 140$ GeV/c^2, $M_{\rm Higgs} = 300$ GeV/c^2 and $\alpha_s(M^2_{Z^0}) = 0.12$.
D. Bardin et al., ${}_{ZF}I^{T}T_{E_R}$ *An Analytical Program for Fermion Pair Production in* e^+e^- *Annihilation*, CERN–TH. 6443/92.

[23] OPAL Collab., G. Alexander et al., Phys. Lett. B262 (1991) 341.

[24] B. Schumm, Y. Dokshitzer, V. Khoze and D. Koetke, Phys. Rev. Lett. 69 (1992) 3025.

[25] OPAL Collab., P. Acton et al., Z. Phys. C53 (1992) 539.

[26] OPAL Collab., G. Alexander et al., Phys. Lett. B264 (1991) 467.

[27] OPAL Collab., P. Acton et al., *Measurement of the Average b Hadron Lifetime in* Z^0 *Decays*, CERN-PPE/93-92, submitted to Z. Phys. C.

[28] OPAL Collab., P. Acton et al., *The Forward-Backward Asymmetry of* $e^+e^- \to b\bar{b}$ *and* $e^+e^- \to c\bar{c}$ *Using Leptons in Hadronic* Z^0 *Decays*, CERN-PPE/93-78, Submitted to Z. Phys. C.

[29] N. Isgur, D. Scora, B. Grinstein and M. Wise, Phys. Rev. D45 (1989) 799.

[30] L. Lyons, D. Gibaut and P. Clifford, Nucl. Instr. and Meth. A270 (1988) 110.